ISBN: 978-3-95450-184-7 doi:10.18429/JACoW-IPAC2018-THPAK030

STUDIES OF LONGITUDINAL DYNAMICS IN THE MICRO-BUNCHING INSTABILITY USING MACHINE LEARNING

T. Boltz*, M. Brosi, E. Bründermann, P. Schönfeldt, M. Schwarz†, M. Yan and A.-S. Müller
Karlsruhe Institute for Technology, Karlsruhe, Germany

Abstract

The operation of synchrotron light sources with short electron bunches increases the emitted coherent synchrotron radiation (CSR) power in the THz frequency range. However, the spatial compression leads to complex longitudinal dynamics, causing the formation of micro-structures in the longitudinal bunch profiles. The fast temporal variation and small scale of these micro-structures put challenging demands on their observation. At the KIT storage ring KARA (Karlsruhe Research Accelerator), diagnostics have been developed allowing direct observation of the dynamics by an electro-optical setup, and indirect observation by measuring the fluctuation of the emitted CSR. In this contribution, we present studies of the micro-structure dynamics on simulated data, obtained using the numerical Vlasov-Fokker-Planck solver Inovesa. To deal with generated data sets in the order of terabytes in size, we apply the machine learning technique k-means to identify the dominant micro-structures in the longitudinal bunch profiles. Following this approach, new insights on the correlation of the CSR power fluctuation to the underlying longitudinal dynamics can be gained.

INTRODUCTION

Due to the self-interaction with its own CSR, short electron bunches in a storage ring are subject to complex longitudinal dynamics. Above a given threshold current, this results in the formation of dynamically changing, but persistent, micro-structures within the electron bunch. As the longitudinal charge distribution varies, this also leads to major fluctuations in the emitted CSR power and is thus called micro-bunching instability. Experimental observations of this phenomenon have been made at various synchrotron light sources, including e.g. [1–3]. Additionally, the underlying longitudinal dynamics can be simulated by numerically solving the Vlasov-Fokker-Planck equation, where the CSR self-interaction can be added as a perturbation to the Hamiltonian. Such theoretical studies have been primarily focused on prediction of the threshold current, leading e.g. to the formulation of an empirical scaling law [4].

This contribution focuses explicitly on the longitudinal dynamics above the threshold current and places special emphasis on the characteristics of the occurring micro-structures. Therefore, the dynamics are simulated for a given machine setting across multiple bunch currents using the in-house developed simulation code Inovesa [5]. Considering the requirements for reasonable temporal and spatial resolution, simulation of the longitudinal dynamics quickly accumulates to large sets of data. In order to explore the generated data, we apply the machine learning method k-means to identify the dominant micro-structures within the longitudinal profiles of a given bunch current. In this contribution, the application of the k-means method is aimed at describing the dynamically changing bunch profiles by merely a few discrete states. The cluster separation is therefore expected to be rather low (e.g. silhouette scores of $S_k \approx 0.5$). Nevertheless, it can still yield very useful information in regard of understanding the underlying dynamics.

While the first part deals with the identification of the dominant micro-structures on the longitudinal bunch profiles within a fixed current and their correlation to the fluctuating emission of CSR power, the second part extends the scope to studies of the micro-structure characteristics across different bunch currents and machine settings.

ANALYSIS OF MICRO-STRUCTURE DYNAMICS

In the studies of the longitudinal dynamics in the micro-bunching instability, it was found that two major regimes exist above the threshold current [6]. In the regular bursting regime directly above the threshold, the CSR power signal

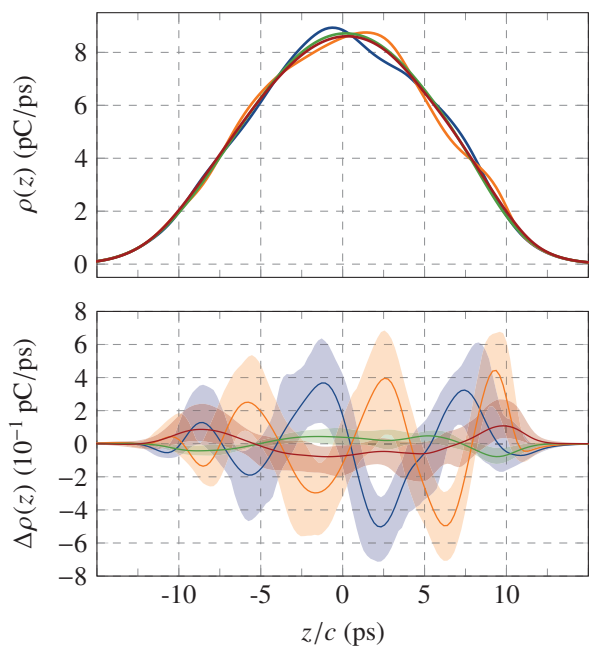

Figure 1: Cluster centers found on the longitudinal profiles for an exemplary bunch current (I_{ex} = 1.15 mA) in the sawtooth bursting regime. Different colors indicate the respective cluster.

* tobias.boltz@kit.edu
† now at CERN, Geneva, Switzerland

ISBN: 978-3-95450-184-7 doi:10.18429/JACoW-IPAC2018-THPAK030

has an almost sinusoidal shape, whereas in the sawtooth bursting regime at higher currents, distinct burst of CSR emission can be observed. The results of the aforementioned application of the k-means method will be discussed for an exemplary bunch current ($I_{ex} = 1.15\,\mathrm{mA}$) within the sawtooth bursting regime.

In the upper part of Fig. 1, the cluster centers found by the k-means method searching for four clusters in the longitudinal bunch profiles are shown. Here, two of four cluster centers (line color blue and orange) display distinct modulations on the longitudinal profiles. An elegant way to emphasize these modulations, is to subtract from each cluster center the global mean profile (calculated over all longitudinal profiles) as shown in the lower part of the figure. Here, the cluster centers are clearly distinguishable and, in the case of the blue and orange cluster, display the phase and paraphase of an almost sinusoidal modulation on the longitudinal profiles. Additionally, the shaded areas denote the standard deviations of the longitudinal profiles within the respective cluster, showing to which degree the cluster centers concur with the actual longitudinal profiles in the respective cluster. In contrast, the red and green cluster centers describe mainly longitudinal profiles with different bunch lengths. This is for example indicated by the slightly higher values of the red cluster center (corresponding to a longer bunch) at the edges of the profile.

Furthermore, the correlation of these findings with the emitted CSR power can be studied. During the clustering procedure, each longitudinal profile $\rho(z, t_i)$, corresponding to the specific time step t_i, is assigned with a cluster label $y(t_i)$. This temporal sequence of integers $y(t_i)$ contains the entire information about the generated clustering results and can be mapped to the corresponding sequence of CSR power values $P_{csr}(t_i)$. This is illustrated in Fig. 2, where each value of $P_{csr}(t_i)$ is colored according to the corresponding cluster label $y(t_i)$ of this time step.

Obviously, the blue and orange cluster contain the longitudinal profiles corresponding to the four distinct bursts of CSR emission, while the red and green cluster describe the phases in between. The points of maximal CSR emission are thus perfectly coinciding with the occurrence of micro-

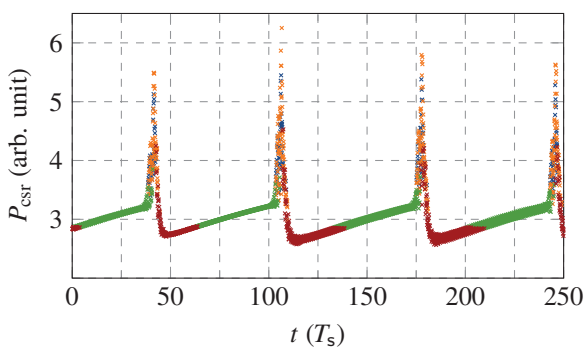

Figure 2: Color-coded CSR power, displaying the correlation between the found modulations on the longitudinal profiles and fluctuations in the emitted CSR.

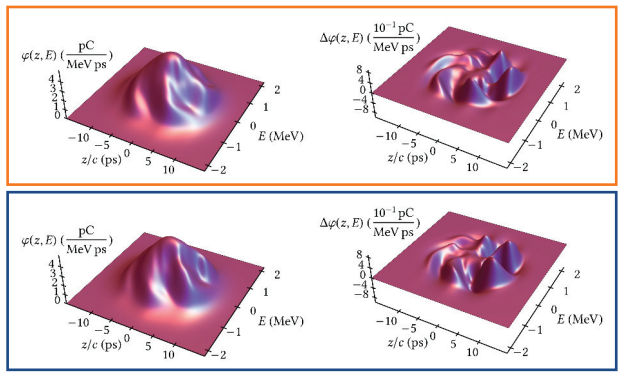

Figure 3: Phase space cluster means (left) corresponding to the blue and orange cluster centers displayed in Fig. 1. To emphasize the occurring micro-structures, the global mean over all phase space densities is subtracted (right).

structures with high amplitude. Between these bursts of emitted CSR, there are transition periods of the longitudinal dynamics where the bunch length reduces gradually.

As the entire longitudinal phase space density can be obtained from simulation, the found micro-structures can be studied directly in phase space. One way to do so, is to calculate the mean phase space density within the found clusters, as displayed in Fig. 3 for the blue and orange cluster. Similarly to the above, in order to emphasize the dynamic structure, the global mean phase space density is subtracted. Here, several distinct micro-structures are visible. By comparison to the results presented in Fig. 1, it can be inferred that the highest values in the amplitude of the modulation on the longitudinal profiles originate from multiple maxima in the phase space density that get added up in the projection on the z-axis. Due to synchrotron motion, the phase space density is rotating and thus leading to an oscillation between phase and paraphase of the modulation on the longitudinal profile.

Although the observed CSR power signal changes significantly with increasing bunch current, micro-structures of similar appearances were found for all currents above threshold, including the regular bursting regime. While the general appearance, i.e. the number of structures and their overall shape, is consistent throughout the different regimes of CSR emission, the temporal changes of their amplitude are the main reason for the differences in emitted CSR power.

MICRO-STRUCTURE CHARACTERISTICS

In order to study the micro-structure characteristics across different bunch currents, the cluster centers found by the k-means method are further analyzed to determine the main frequency f_{mod} and amplitude A_{mod} of the modulation on the longitudinal profiles, as shown in Fig. 4. For the simulated wide bunch current range from 0.5 mA to 2.0 mA, the modulation frequencies are distributed mainly around two levels. While the modulation frequencies around 50 GHz

ISBN: 978-3-95450-184-7 doi:10.18429/JACoW-IPAC2018-THPAK030

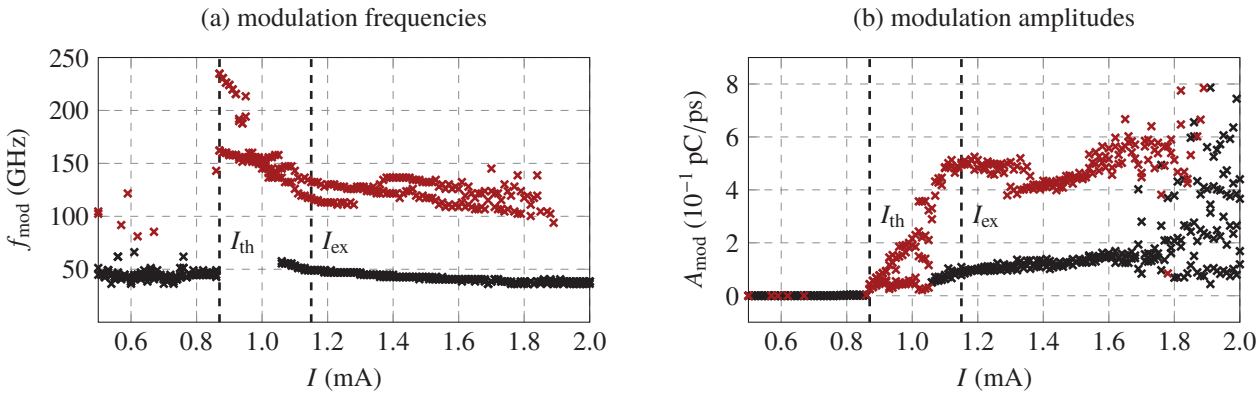

Figure 4: Modulation frequencies (a) and amplitudes (b) across different currents. As higher frequencies correspond to modulations caused by micro-structures in phase space, values higher than 75 GHz are colored red. The same color scheme is then applied to the displayed modulation amplitudes.

correspond to cluster centers describing mainly changes in bunch length, the higher frequencies correspond to distinct micro-structures on the longitudinal profiles. The latter start occurring directly above the threshold I_{th} and stay around a slightly decaying value. Despite the slight decay, which is mainly caused by bunch lengthening, the number of micro-structures is still the same for all these currents.

The amplitude of the micro-structures (Fig. 4b) starts rising directly above the threshold current until reaching a saturation value at $I \approx 1.1$ mA. Eventually for $I > 1.8$ mA, the amplitudes of modulations due to changes in bunch length are in the same magnitude as those caused by the micro-structures.

While the number of micro-structures in phase space is found to be constant across different currents for a given set of machine parameters, this no longer holds for modifications of specific parameters e.g. synchrotron frequency or the height of the vacuum gap $g = 2h$. Figure 5 shows the results of systematic simulations for different vacuum gaps. Compared to the formulation found by K.F.L. Bane et al. [4] for the threshold current, the number of micro-structures n_{str} and modulation frequency f_{mod} show interestingly the same dependence on the vacuum gap, i.e. linear to $h^{-1.5}$. Additionally it should be noted, while the number of micro-structures is assumed to be a discrete quantity and counted directly by studying phase space, the modulation frequency is not necessarily bound to the same constraints. Nevertheless, the modulation frequency decreases stepwise with increasing height of the vacuum gap, indicating an intrinsic discretization of the occurring micro-bunching.

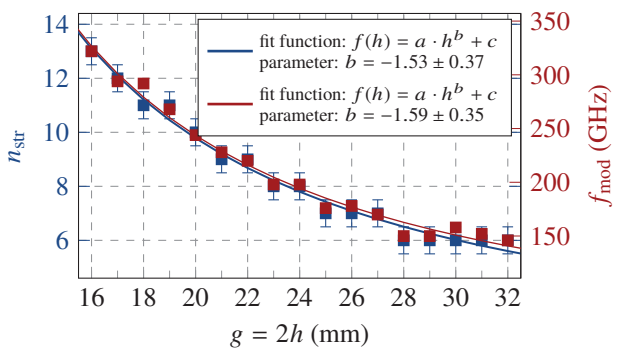

Figure 5: Number of micro-structures n_{str} and modulation frequencies f_{mod} for different vacuum gaps $g = 2h$.

SUMMARY AND OUTLOOK

The longitudinal dynamics in the micro-bunching instability can be studied on simulation data using the Vlasov-Fokker-Planck Solver Inovesa. Careful analysis of the obtained data led to new insights on the underlying dynamics, e.g. the number of micro-structures in phase space is observed to be constant above the threshold for otherwise fixed machine settings. Additionally, dependency of further characteristics of the micro-structures on various machine parameters has been found, which coincides with the established formulation for the bursting threshold. This interesting finding might stimulate further understanding of the micro-bunching instability.

ACKNOWLEDGEMENT

T. Boltz, M. Brosi and P. Schönfeldt want to acknowledge the support by the Helmholtz International Research School for Teratronics (HIRST).

REFERENCES

[1] M. Abo-Bakr et al., PAC'03 **5**, 3023-3025 (2003).

[2] W. Shields et al., *Journal of Physics: Conference Series* **357**, 012037 (2012).

[3] C. Evain et al., *EPL (Europhysics Letters)* **98**, 40006 (2012).

[4] K.L.F. Bane et al., *Phys. Rev. ST Accel. Beams* **13**, 104402 (2010).

[5] P. Schönfeldt et al., *Phys. Rev. Accel. Beams* **20**, 030704 (2017).

[6] T. Boltz, Master's Thesis, doi: 10.5445/IR/1000068253 (2017).